processes including the Wnt/β-catenin signaling pathway [15,16]. GSK-3β inhibits the Wnt/β-catenin signaling pathway by phosphorylating β-catenin to accelerate its proteolysis [15,17], resulting in the inhibition of transcription of *CCND1*, *c-myc* and other Wnt target genes. In addition, GSK-3β phosphorylates cyclin D1 to promote its degradation. Accordingly, GSK-3β reduces cyclin D1 expression by two mechanisms: inhibition of *CCND1* gene transcription and promotion of cyclin D1 protein degradation [17,18]. Therefore, we thought the compounds that induce GSK-3β activation could be useful as anti-tumor agents.

We previously reported that differentiation-inducing factors (DIF-1 and DIF-3), which were identified in *Dictyostelium discoideum* as putative morphogens required for stalk cell differentiation [19,20], have a powerful antiproliferative effect on human cancer cell lines *in vitro* [21–27]. With regard to the underlying mechanisms, we revealed that DIFs accelerated degradation of cyclin D1 and β-catenin through the activation of GSK-3β, leading to the suppression of the Wnt/β-catenin signaling pathway and cell cycle arrest at the G_0/G_1 phase in various human cells [21–26]. Surprisingly, DIF-1 also suppressed proliferation of colon cancer cells in which the Wnt/β-catenin signaling pathway was constitutively activated by lack of β-catenin destruction mechanisms. In this regard, we revealed that DIF-1 suppressed transcription factor 7-like 2 (TCF7L2) expression via reduced early growth response-1 (Egr-1) protein amount, thereby inhibiting the Wnt/β-catenin signaling pathway without affecting β-catenin expression level [27]. However, the mechanisms for DIF-1's *in-vivo* action remain to be clarified.

Therefore, in the present study, to assess whether DIF-1 is applicable to the treatment of malignant tumors, we examined its *in-vivo* effects using mice. First, we examined its pharmacokinetics and toxicity. Second, we evaluated the anti-cancer effects of DIF-1 using a spontaneous cancer model and human cancer xenograft models. For the former, we employed *Mutyh*-deficient (*Mutyh*$^{-/-}$) mice, which lack the MutY homolog (MUTYH), a mammalian DNA glycosylase that initiates base excision repair, and is thus susceptible to oxidative stress-induced carcinogenesis [28–31]. These mice provide a useful animal model for examining colorectal adenoma and carcinoma [31]. For the latter, we used nude mice bearing HCT-116 cells and those bearing HeLa cells. Using these cancer models, we show for the first time that orally administered DIF-1 exhibits anti-tumor effects *in vivo*. Third, we examined the mechanisms for DIF-1's *in-vivo* actions.

2. Materials and methods

2.1. Chemicals and antibodies

DIF-1 (1-(3,5-dichloro-2, 6-dihydroxy-4-methoxyphenyl)-1-hexanone) was synthesized as described previously (purity: >98%) [32]. Celecoxib was kindly provided by Pfizer (New York, NY, USA). An anti-cyclin D1 polyclonal antibody was purchased from Santa Cruz Biotechnology (Santa Cruz, CA, USA). Anti-β-catenin and anti-GSK-3β monoclonal antibodies were purchased from R&D Systems (Minneapolis, MN, USA). Anti-Egr-1 monoclonal antibody, anti-transcription factor 7-like 2 (TCF7L2) monoclonal antibody (6H5-3) and anti-phospho-GSK-3β (Ser^9) polyclonal antibody were purchased from Cell Signaling Technology (Danvers, MA, USA). An anti-GAPDH monoclonal antibody was purchased from Abcam (Cambridge, MA, USA). An anti-α-tubulin monoclonal antibody was purchased from Calbiochem (Darmstadt, Germany). Growth factor-reduced Matrigel was obtained from BD Biosciences (San Jose, CA, USA).

2.2. Cell culture

HCT-116 and HeLa cells were grown in Dulbecco's modified Eagle's medium (Sigma, St. Louis, MO, USA) supplemented with 10% fetal bovine serum, 100 U/mL penicillin G, and 0.1 μg/mL streptomycin.

2.3. Western blot analysis

Protein samples (10 μg/lane) were separated by 12% SDS–polyacrylamide gel electrophoresis and then transferred to a polyvinylidene difluoride membrane using a semi-dry transfer system (1 h at 12 V). Western blot analysis was performed as described previously [21]. Optical densitometric scans were performed using NIH Image J software.

2.4. Administration of DIF-1

For intraperitoneal administration, 30 mg/kg DIF-1, pounded in a mortar and suspended in PBS, was injected into the abdomens of C57BL/6J male mice (10–11 weeks old; Kyudo, Tosu, Japan). For oral administration, DIF-1 was suspended in a 0.25% methylcellulose solution or dissolved in soybean oil. These DIF-1-containing solutions were then orally administered to the C57BL/6J mice.

2.5. Measurement of the DIF-1 concentration in mouse plasma

Mouse blood samples were collected by cardiac puncture at the indicated times, and plasma was isolated by centrifugation at 500 × *g* for 15 min. The plasma concentration of DIF-1 was determined by a reverse phase high-performance liquid chromatography (HPLC) system (Waters 2695, Milford, MA, USA) as described previously [33] with a slight modification. Briefly, mouse plasma samples (200 μL) containing 500 ng daisein (Wako Pure Chemical Industries Ltd., Osaka, Japan) as an internal standard were mixed with 200 μL chloroform. After mixing, the solution was centrifuged at 13,000 × *g* for 5 min, and then the organic phase was separated and evaporated. The residue was dissolved in 80 μL of a mixture of acetic acid (5%, v/v) and methanol (40%, v/v). A sample (50 μL) was then applied to a column for separation (TSKgel ODS-80Ts; Tosoh Corporation, Tokyo, Japan). The samples were eluted by a linear gradient of methanol (40–95%) in the presence of 5% acetic acid over 40 min at a flow rate of 1.0 mL/min. A UV detector was operated at 277 nm. A calibration curve was prepared by plotting the area ratios of DIF-1 normalized to the internal standard.

2.6. Intestinal tumor model mice

Intestinal tumors (adenomas and carcinomas) were formed by methods reported previously with slight modifications [31]. Briefly, $KBrO_3$ dissolved in drinking water at a concentration of 2 g/L was provided to 4-week-old mice for 12 weeks. At 16 weeks of age, the mice were randomly divided into six groups (six mice including three males and three females in each group). Mice in test groups were orally administered with DIF-1 or celecoxib, which was suspended in a 0.25% methylcellulose solution, once a day for 5 days/week over 4 weeks. Control mice received the vehicle only. The body weight of the mice was monitored weekly. At 20 weeks of age, all mice were sacrificed to obtain blood and intestinal samples. Blood samples were analyzed by a Celltac-alpha MEK-6358 (Nihon Kohden, Tokyo, Japan) for blood cell counts. Intestines were fixed in 4% formaldehyde, and the tumors were observed under a microscope. Images of the tumors were obtained and analyzed using NIH Image J software. For Western blot analysis, intestinal tissues (2 cm down from the pylorus) were homogenized in Laemmli's sample buffer immediately after

resection. After adjustment of the protein content, the samples were electrophoresed and blotted with antibodies. Intestinal bleeding was examined in excrement by the guaiac reaction (Sionogi II test; Sionogi, Osaka, Japan).

2.7. Human cancer xenograft model mice

Eight-week-old female mice (BALB/c nu/nu) were subcutaneously injected in their right flank with 400 μL Matrigel and 5×10^6 human cancer cells (HCT-116 or HeLa) suspended in PBS (1:1, v:v). Mice were randomly divided into DIF-1 treatment and control groups. At the beginning, DIF-1 was suspended in a 0.25% methylcellulose solution and orally administered as in the experiment with intestinal tumor model mice. However, later, we improved the administration method to elevate plasma concentrations of DIF-1 by dissolving DIF-1 in soybean oil and dosing every 12 h (300 mg/kg in the morning and 150 mg/kg in the evening) for 5 days/week. Control group mice received the vehicles only. The body weight of mice was monitored weekly. Tumors removed on the indicated days were measured for size and weight, and then prepared for Western blot analysis. Blood samples were collected and analyzed for blood cell counts.

2.8. Statistical analysis

Results are expressed as the means ± s.e.m. Statistical analyses of differences between two mean values were performed using the Student's *t*-test. Multiple mean values were compared by one-way ANOVA with the Dunnett's multiple comparison test.

2.9. Ethics information

The study protocol was approved by the Committee of Ethics on Animal Experiments at Kyushu University (Permit Number: A22-046-0). Animal handling and procedures were carried out in compliance with the Guidelines for Animal Experiments, Kyushu University, and the Law (No. 105) and Notification (No. 6) of the Japanese Government. All surgeries were performed under sodium pentobarbital anesthesia, and all efforts were made to minimize suffering.

3. Results

3.1. Plasma concentration of DIF-1 in mice

To examine whether plasma DIF-1 concentrations reach levels that can show an antiproliferative effect on tumor cells, we measured DIF-1 concentrations after intraperitoneal and oral administration in wild-type C57BL/6J mice using a HPLC system. After intraperitoneal injection, the DIF-1 concentration rapidly increased and reached maximal levels (20–30 μg/mL) within 30 min, followed by a rapid decline (Fig. 1A). When orally administered, the DIF-1 concentration reached maximal levels (30–40 μg/mL) within 1 h, and the decline was much slower compared with that following intraperitoneal injection (Fig. 1B). Because the EC_{50} value of DIF-1 for an *in vitro* antiproliferative effect is 5–8 μg/mL, these results suggest that the plasma concentration of DIF-1 can be sufficiently elevated to show an

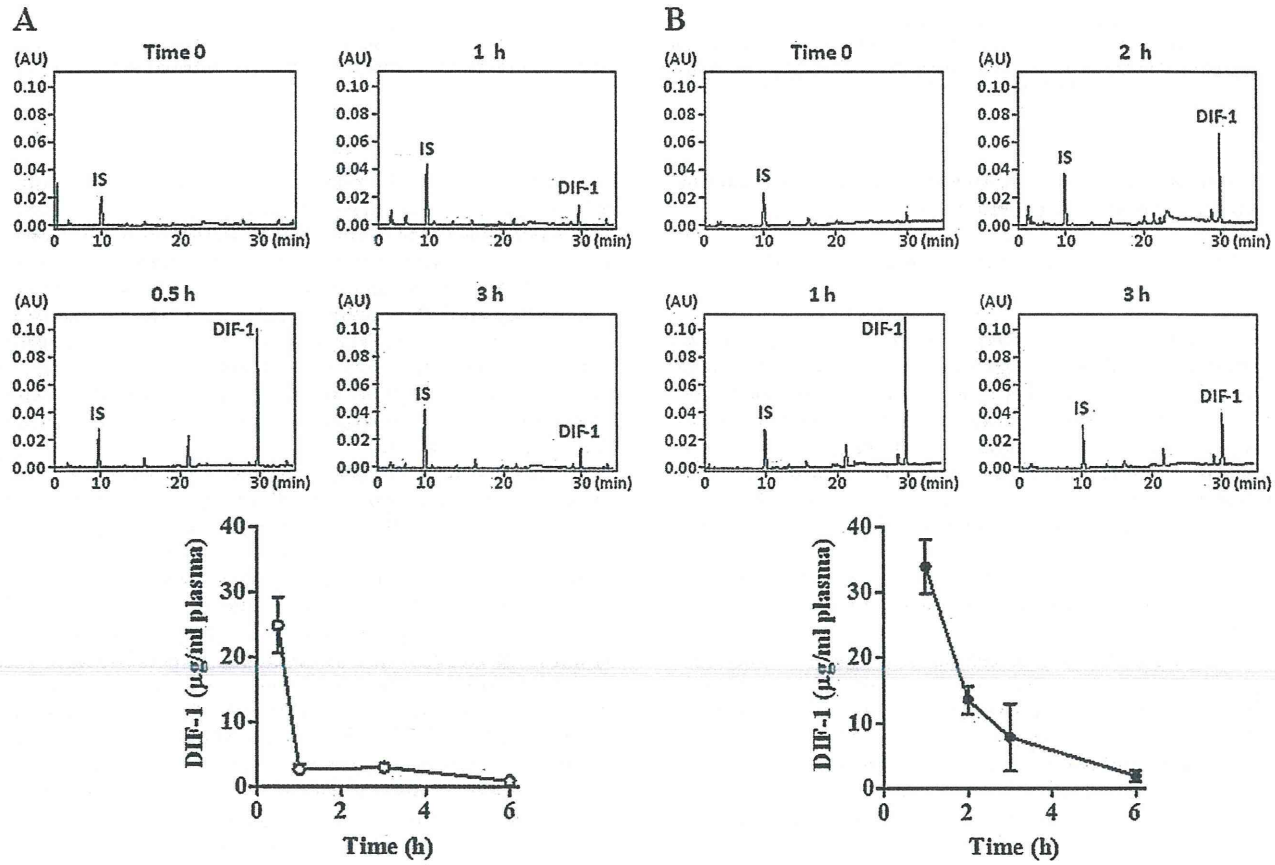

Fig. 1. Plasma concentrations of DIF-1.
DIF-1 was administered to mice intraperitoneally (A) or orally (B). Blood was collected at the indicated times to prepare HPLC samples. Upper panels: HPLC elution profiles. Lower panels: time course of plasma DIF-1 concentrations. Values are the means ± s.e.m. ($n = 3$). IS, internal standard.

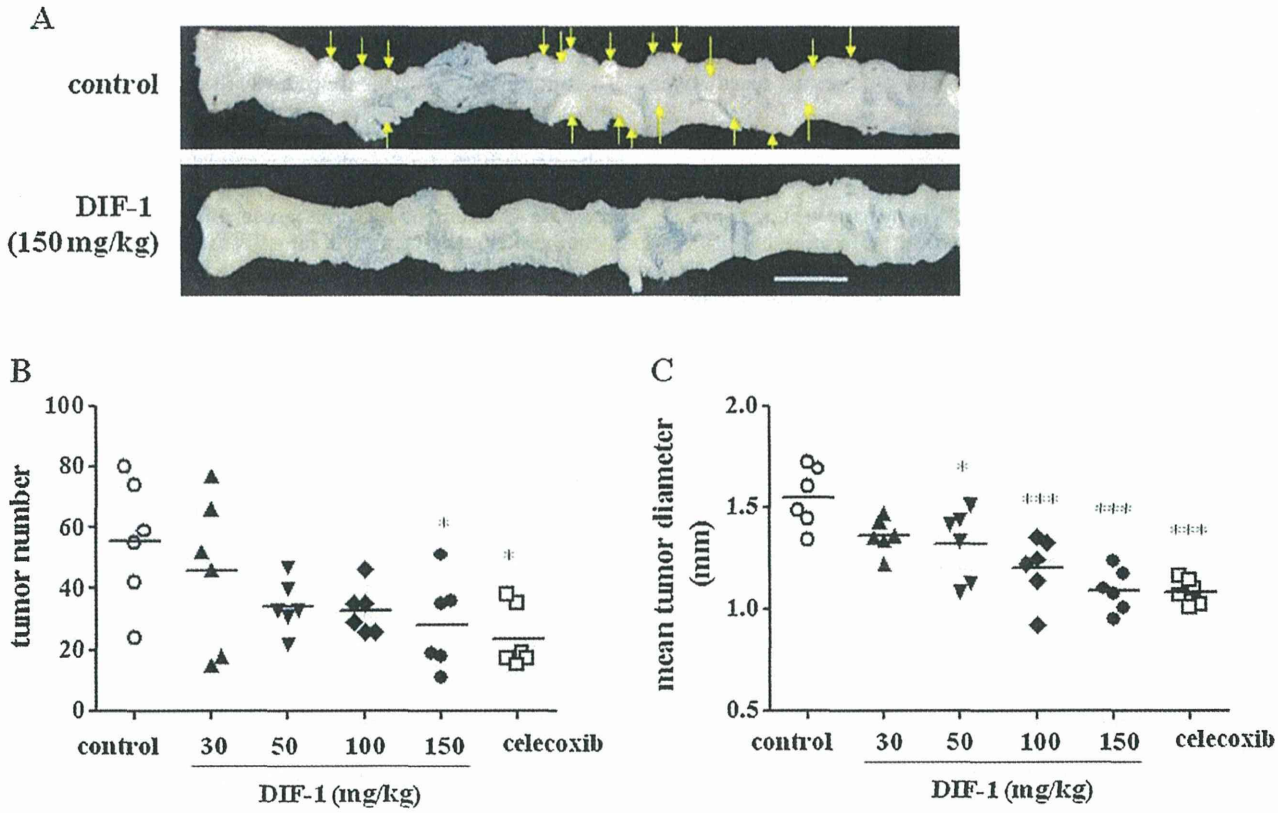

Fig. 2. Effect of DIF-1 on intestinal tumors induced by $KBrO_3$ in *Mutyh*$^{-/-}$ mice.
A. Proximal region of the small intestines. Scale bar indicates 1 cm. Arrows indicate tumors with a >2.5 mm diameter. B. Tumor numbers are plotted for each mouse. Horizontal bars indicate the means of each group ($n = 6$). C. Mean tumor diameters are plotted for each mouse. Horizontal bars indicate the means of each group ($n = 6$). $^{*}P < 0.05$ vs. control, $^{***}P < 0.001$ (one-way ANOVA with Dunnett's multiple comparison test).

antiproliferative effect *in vivo*. Therefore, we used oral administration for the following experiments.

3.2. Effect of DIF-1 on oxidative stress-induced tumors in *Mutyh*$^{-/-}$ mice

To evaluate the anti-tumor effect of DIF-1 *in vivo*, we first used mice deficient for MUTYH, an enzyme that prevents formation of oxidative stress-induced DNA lesions. Studies have shown that MUTYH deficiency might be involved in the development of colorectal adenoma and carcinoma in humans [28–30]. As we reported previously [31], the occurrence of carcinomas in the small intestine was dramatically increased by oxidative stress in *Mutyh*$^{-/-}$ mice. Twelve weeks of treatment with 0.2% $KBrO_3$, a strong oxidant, followed by vehicle treatment for 4 weeks induced numerous intestinal tumors (55.7 ± 8.4, $n = 6$) in *Mutyh*$^{-/-}$ mice, whereas only a small number of tumors were formed in wild-type mice (1.2 ± 0.5, $n = 6$).

We administered DIF-1 or celecoxib to *Mutyh*$^{-/-}$ mice for 4 weeks to examine the effects of these compounds. We used celecoxib for reference because it has been used for the treatment of FAP patients [34]. DIF-1 treatment (10–150 mg/kg/day for 4 weeks) markedly reduced the number and size of intestinal tumors in a dose-dependent manner (Fig. 2A–C). The effectiveness of DIF-1 appeared to be comparable with that of celecoxib, because the same doses (150 mg/kg) of these compounds showed similar effects.

Next, we carried out Western blot analyses of tumor samples obtained from vehicle- or DIF-1 (150 mg/kg)-treated mice. Because DIF-1 activates GSK-3β by dephosphorylation of Ser^9 in cultured cells [22,23,25], we analyzed the effect of DIF-1 on the phosphorylation status of GSK-3β Ser^9 in the intestines. As shown in Fig. 3A, DIF-1 significantly decreased the phosphorylation level of GSK-3β Ser^9, suggesting that DIF-1 also activated GSK-3β *in vivo*. Furthermore, DIF-1 markedly decreased the protein expression levels of Egr-1, TCF7L2 and cyclin D1, although β-catenin levels were unaltered (Fig. 3B). These results suggested that DIF-1 inhibited tumor growth in *Mutyh*$^{-/-}$ mice by GSK-3β-mediated suppression of cyclin D1 expression and Egr-1-mediated suppression of TCF7L2 expression.

To examine whether long-term treatment with DIF-1 shows adverse effect on the general condition, we measured their body weight and peripheral blood cell counts, as well as observing their appearance and activity. Red blood cell (RBC) numbers and hemoglobin (Hb) concentrations were significantly lower in *Mutyh*$^{-/-}$ mice compared with those in wild-type mice (Table 1). *Mutyh*$^{-/-}$ mice may have suffered from anemia caused by intestinal bleeding due to developed tumors, because excrement from *Mutyh*$^{-/-}$ mice was strongly positive (+++) for occult blood, whereas excrement from wild-type mice was negative (data not shown). There were no significant differences in white blood cell (WBC) or platelet numbers and changes in body weight (ΔBW) between *Mutyh*$^{-/-}$ mice and wild-type mice. Administration of DIF-1 or celecoxib did not affect the appearance, activity, WBC and platelet numbers, or ΔBW of the mice. However, DIF-1 and celecoxib significantly increased RBC counts and Hb levels, suggesting that these compounds prevent bleeding from the intestinal mucosa by reducing size and number of tumors (Table 1).

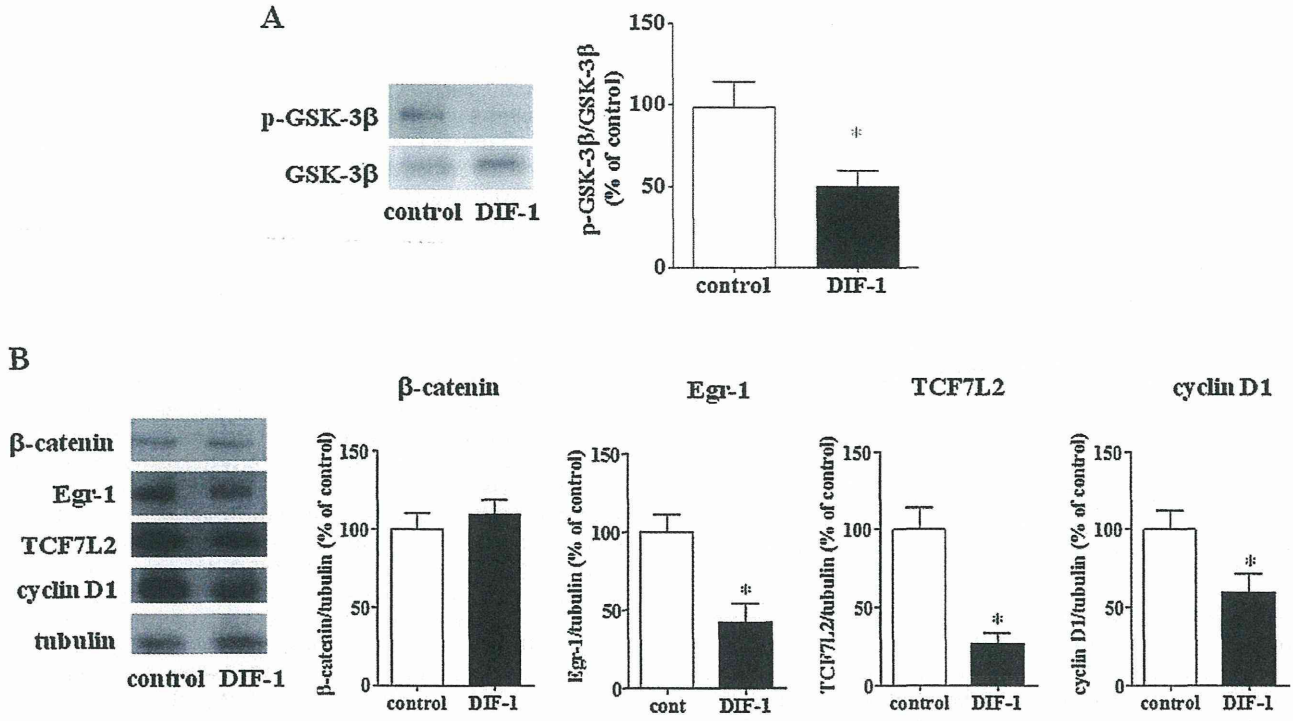

Fig. 3. Western blot analyses of proteins extracted from *Mutyh*$^{-/-}$ mouse small intestines.
Protein samples prepared from the small intestines of vehicle- and DIF-1 (150 mg/kg)-treated mice were analyzed by Western blotting. A. GSK-3β phosphorylation levels. Protein samples were subjected to Western blotting to analyze phosphorylation of GSK-3β Ser^{9} using an anti-phospho-GSK-3β antibody. After stripping, the membranes were reprobed with an anti-GSK-3β antibody. Band densities are shown as percentages of the controls. Values are the means ± s.e.m. (n = 6). *P < 0.05 vs. control (Student's t-test). p-GSK-3β, phospho-GSK-3β. B. Expression levels of β-catenin, Egr-1, TCF7L2, and cyclin D1. Band densities were quantified and normalized to those of tubulin. Values are the means ± s.e.m. (n = 6). *P < 0.05 vs. control (Student's t-test).

3.3. *Effect of DIF-1 on human cancer xenografts*

Our experiments using *Mutyh*$^{-/-}$ mice showed that DIF-1 inhibited intestinal tumor growth. However, it appeared possible that DIF-1 administered into the digestive tract directly acted on the intestinal mucosa without absorption into systemic circulation. Therefore, we investigated whether orally administered DIF-1 could show an anti-tumor effect on tumors growing in a region distant from the digestive tract. For this purpose, we employed nude mice xenografted with two different cell species of human cancer: HCT-116-xenografted mice to examine the effect of DIF-1 on colon cancer *in vivo* and HeLa-xenografted mice to confirm the effect of DIF-1 in a different cancer. One reason that we chose these two cancer cell species was that the β-catenin destruction mechanism is mutated in HCT-116 but it is intact in HeLa cells. We first treated these xenografted mice with orally administered DIF-1 (150 mg/kg every 24 h) that was suspended in 0.25% methylcellulose (the same solvent used in Mutyh$^{-/-}$ mice experiments). However, DIF-1 failed to show a significant effect on tumor xenografts (data not shown). We considered that this

Table 1
Effects of DIF-1 on blood cell counts and body weight.

		WBC (×10^2 cells/μL)	RBC (×10^4 cells/μL)	Hb (g/dL)	Plt (×10^4 cells/μL)	ΔBW (g)
Wild-type						
Vehicle		58.0 ± 5.7	923.3 ± 16.3	12.2 ± 0.38	52.7 ± 5.5	3.26 ± 0.77
Mutyh$^{-/-}$						
Vehicle		54.6 ± 6.1	615.7 ± 66.4**	10.0 ± 0.93*	64.7 ± 9.5	1.75 ± 0.36
DIF-1	mg/kg					
	10	50.5 ± 6.6	678.8 ± 60.0**	10.6 ± 0.38	65.0 ± 7.9	1.85 ± 0.53
	30	43.7 ± 7.2	682.3 ± 67.0**	11.0 ± 0.69	74.3 ± 5.3	1.87 ± 0.36
	100	65.2 ± 13.1	752.0 ± 34.7	11.6 ± 0.40	58.4 ± 3.9	1.93 ± 0.50
	150	55.9 ± 4.1	787.3 ± 37.7	11.7 ± 0.41	73.0 ± 7.0	2.16 ± 0.66
Celecoxib	mg/kg					
	150	53.5 ± 12.7	828.3 ± 29.1	11.6 ± 0.38	64.1 ± 6.6	2.51 ± 0.53

DIF-1, celecoxib or the vehicle (methylcellulose) was orally administered to mice for 4 weeks. Data represent the means ± s.e.m. Statistical significance was determined by one-way ANOVA with Dunnett's multiple comparison test. N = 6 for each group. WBCs, white blood cells; RBCs, red blood cells; Hb, hemoglobin; Plt, platelets; ΔBW, body weight change from 12 to 16 weeks.
* P < 0.05 vs. vehicle-treated wild-type mice.
** P < 0.01 vs. vehicle-treated wild-type mice.

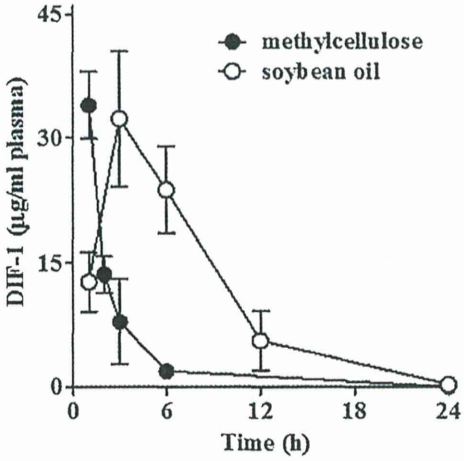

Fig. 4. Improvement of DIF-1 pharmacokinetics by dissolving it in soybean oil. Mice orally received DIF-1 suspended in methylcellulose or dissolved in soybean oil. Blood was collected at indicated times after administration and measured for plasma DIF-1 concentration using an HPLC system. $N = 3$ for each time point. Methylcellulose data (1–6 h) are the same as those shown in Fig. 1B.

observation might result from the difficulty to maintain a sufficient concentration of DIF-1 for more than 3 h (Fig. 1B).

After exploration of a method to increase DIF-1 plasma concentration, we found that soybean oil was a better solvent than methylcellulose. This effect was probably observed because of enhanced absorption, although the trough concentration at 24 h was still very low (Fig. 4). Therefore, we treated tumor-bearing nude mice with DIF-1 dissolved in soybean oil every 12 h (300 mg/kg in the morning and 150 mg/kg in the evening for 5 days/week).

As shown in Fig. 5A, DIF-1 administered in this manner significantly suppressed the growth of HCT-116-xenograft tumor masses and the tumor weight was reduced by approximately 40% compared with that of the controls. Subsequently, we found that the treatment with DIF-1 significantly decreased the phosphorylation levels of GSK-3β Ser^9 (Fig. 5B) and the protein amounts of Egr-1, TCF7L2 and cyclin D1, whereas β-catenin levels were unaltered (Fig. 5C). These results were consistent with our previous ones obtained from *in vitro* experiments using cultured HCT-116 cells, in which DIF-1 strongly inhibited HCT-116 cell proliferation by GSK-3β-mediated degradation of cyclin D1 and suppression of Egr-1 expression, which subsequently inhibited TCF7L2-mediated gene transcription without affecting β-catenin expression [27].

DIF-1 administration also significantly decreased the weight of HeLa-xenograft tumor masses (Fig. 6A). Similarly to HCT-116-xenograft tumors, the treatment with DIF-1 showed tendency to inhibit GSK-3β Ser^9 phosphorylation, although it was not statistically significant (Fig. 6B). DIF-1 treatment significantly decreased the expression of β-catenin, TCF7L2 and cyclin D1 (Fig. 6C), consistent with our previous results obtained using cultured HeLa cells [21,22], indicating that DIF-1 inhibited HeLa-xenograft tumor growth by GSK-3β-mediated degradation of cyclin D1 and suppression of the Wnt/β-catenin signaling pathway.

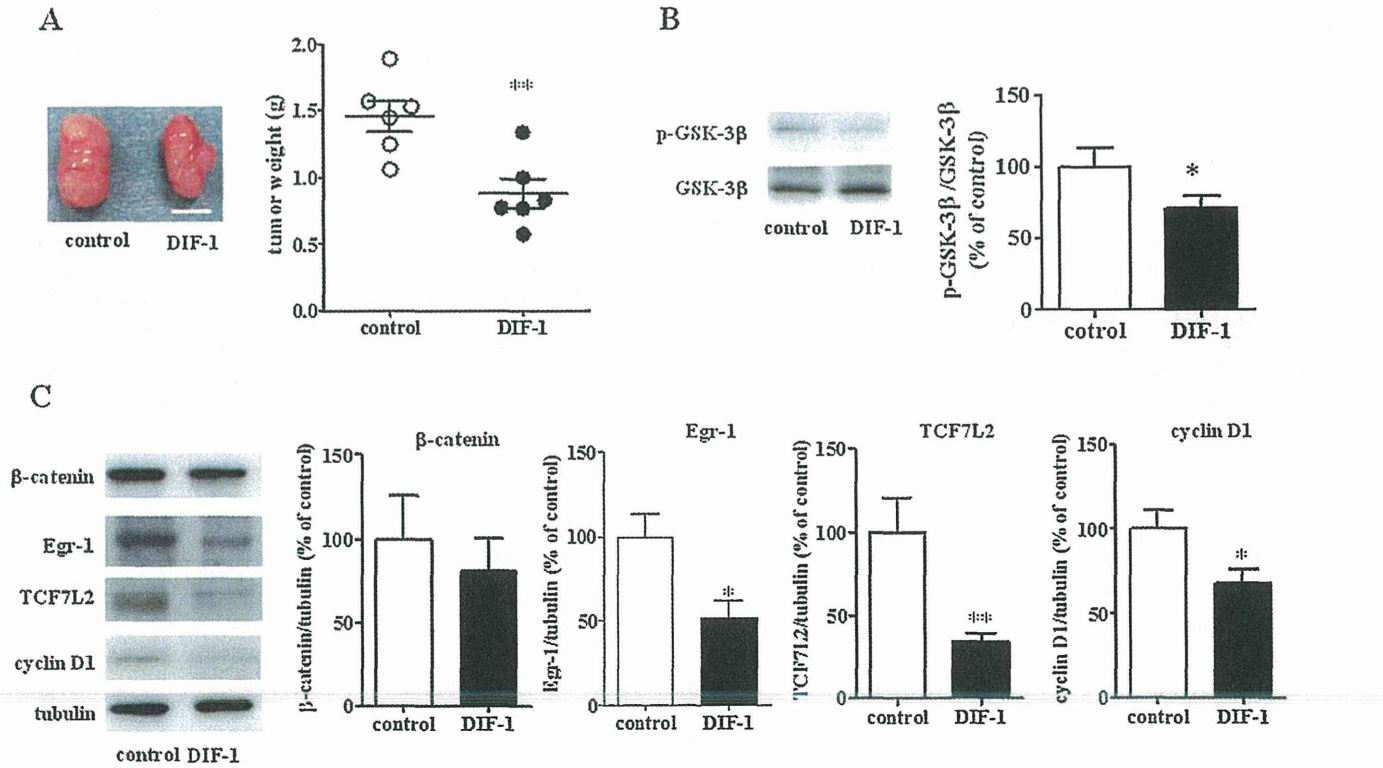

Fig. 5. Effect of orally administered DIF-1 on HCT-116-xenograft tumors.
A. Tumor appearance and weight. HCT-116 cells suspended in Matrigel were subcutaneously injected into the right flanks of mice. Tumor masses were removed after 2 weeks. Photographs show representative tumors isolated from each group of mice. Scale bar indicates 1 cm. Values are the means ± s.e.m. ($n = 6$). *$P < 0.05$ vs. control, **$P < 0.01$ vs. control (Student's t-test). B. GSK-3β phosphorylation levels. Protein samples were prepared from enucleated tumors and analyzed by Western blotting for phosphorylation of GSK-3β Ser^9. The membranes were stripped and then reprobed with an anti-GSK-3β antibody. Band densities are shown as percentages of the controls. Values are the means ± s.e.m. ($n = 6$). *$P < 0.05$ vs. control (Student's t-test). p-GSK-3β, Ser^9 phosphorylated GSK-3β. C. Expression levels of Wnt signaling-related proteins. Protein samples were prepared from enucleated tumors and analyzed by Western blotting for β-catenin, Egr-1, TCF7L2, and cyclin D1. Band densities were quantified and normalized to those of tubulin. Values are the means ± s.e.m. ($n = 6$). *$P < 0.05$ vs. control (Student's t-test).

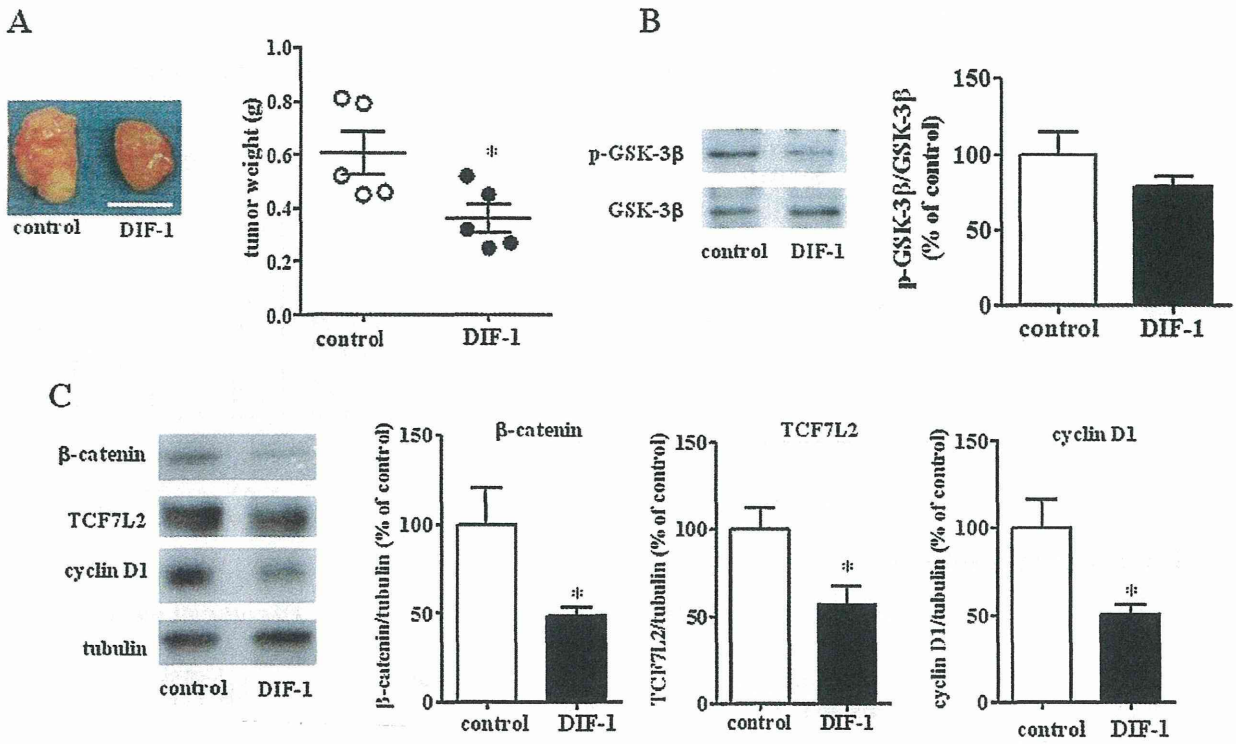

Fig. 6. Effect of orally administered DIF-1 on HeLa-xenograft tumors.
A. Tumor appearance and weight. HeLa cells suspended in Matrigel were subcutaneously injected into the right flanks of mice. Tumor masses were removed after 3 weeks. Photographs show representative tumors isolated from each group of mice. Scale bar indicates 1 cm. Values are the means ± s.e.m. ($n = 5$). *$P < 0.05$ vs. control, **$P < 0.01$ vs. control (Student's *t*-test). B. GSK-3β phosphorylation levels. Protein samples were prepared from enucleated tumors and analyzed by Western blotting for phosphorylation of GSK-3β Ser^9. The membranes were stripped and then reprobed with an anti-GSK-3β antibody. Band densities are shown as percentages of the controls. Values are the means ± s.e.m. ($n = 5$). *$P < 0.05$ vs. control (Student's *t*-test). p-GSK-3β, Ser^9 phosphorylated GSK-3β. C. Expression levels of Wnt signaling-related proteins. Protein samples were prepared from enucleated tumors and analyzed by Western blotting for β-catenin, TCF7L2, and cyclin D1. Band densities were quantified and normalized to those of tubulin. Values are the means ± s.e.m. ($n = 5$). *$P < 0.05$ vs. control (Student's *t*-test).

Finally, we found no significant differences in the appearance, activity, body weight, and blood cell counts between DIF-1-treated mice and the controls, despite the treatment with higher dose of DIF-1 compared with Table 1 (Fig. 7).

4. Discussion

The present study clearly showed for the first time that DIF-1 was absorbed through the digestive tract to elevate its blood concentration and inhibited *in-vivo* tumor growth without manifesting any apparent toxicity in three different cancer model animals, *Mutyh*$^{-/-}$ mice, HCT-116-bearing mice and HeLa-bearing mice, suggesting that this compound might be applicable for the treatment of human cancer. And moreover, regarding the mechanisms for the anti-tumor effect of DIF-1, we found that this compound also induced dephosphorylation of GSK-3β and reduced TCF-mediated gene transcription *in vivo*.

MUTYH is a mammalian DNA glycosylase that initiates base excision repair by excising adenine opposite 8-oxoguanine and 2-hydroxyadenine opposite guanine, thereby preventing G:C to T:A transversion mutations caused by oxidative stress [35–37]. Recently, a biallelic germline mutation of *MUTYH* has been found in humans. Those carrying this *MUTYH* mutation tend to develop multiple adenomatous colon polyps and have an increased risk of colorectal cancer in parallel with an increased incidence of G:C to T:A somatic mutations in the *APC* gene [29,30]. These mutations of the *APC* gene induce constitutive activation of Wnt/β-catenin signaling as observed in FAP patients. This type of polyposis is called MUTYH-associated polyposis (MAP). Therefore, the animal model that we employed appeared to be adequate to evaluate the clinical utility of DIF-1. The efficacy of DIF-1 for treatment of oxidative stress-induced intestinal tumors in *Mutyh*$^{-/-}$ mice was comparable with that of celecoxib, the only non-steroidal anti-inflammatory drug clinically applicable for FAP patients. Because celecoxib and DIF-1 inhibited TCF-mediated gene expression in colon cancer cells [38,39], this may be a mechanism underlying the intestinal tumor growth inhibition by DIF-1 and celecoxib.

Oral administration of DIF-1 suspended in methylcellulose inhibited tumor growth in *Mutyh*$^{-/-}$ mice, whereas at first the same treatment failed to inhibit the growth of xenograft tumors. Although we have not been able to address the precise reason for this failure, we suppose that orally administered DIF-1 might exert direct actions on tumors in the intestinal mucosa without being absorbed into systemic circulation and that the plasma concentration of DIF-1 may not have been sufficient to inhibit growth of the xenograft tumors distant from the digestive tract. It was difficult to maintain a sufficiently high plasma concentration of DIF-1 for longer than 3 h as shown in Fig. 1B. Therefore, we explored another method to improve absorption of DIF-1 and found that soybean oil was a better solvent than methylcellulose to maintain the plasma concentration of DIF-1 (Fig. 4). The reason for this may be that hydrophobic DIF-1 molecules were more soluble in oil than in water. In any case, oral administration of DIF-1 dissolved in soybean oil successfully inhibited growth of the xenograft tumors, which indicated that DIF-1 distributed through systemic circulation could inhibit tumor growth when the plasma concentration of DIF-1 was sufficiently elevated.

The phosphorylation status of GSK-3β Ser^9 indicated that DIF-1 activated or tended to activate this kinase in both *Mutyh*$^{-/-}$ mice and nude mice bearing xenograft tumors. This observation is

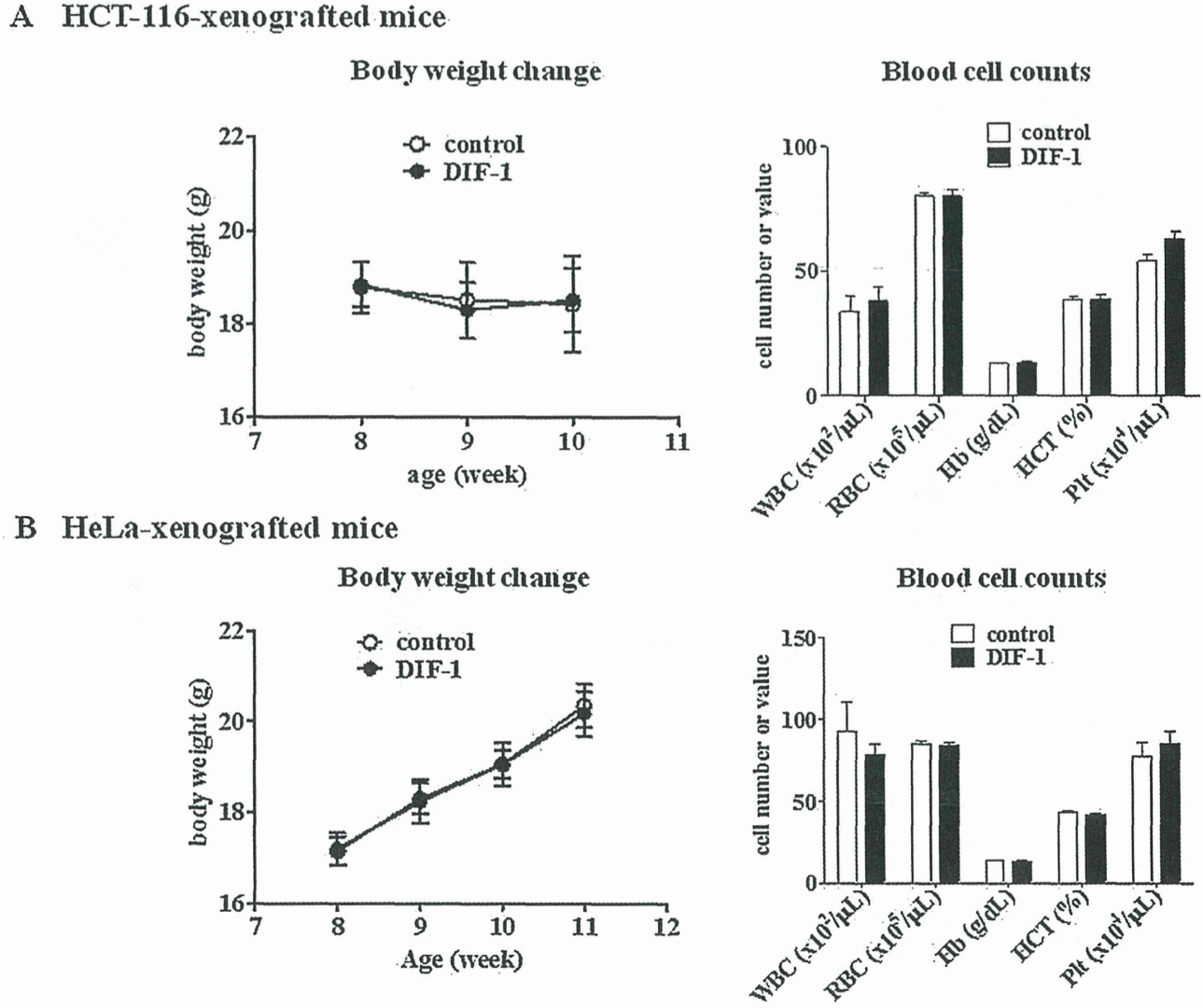

Fig. 7. Effect of DIF-1 on the body weight and blood cell counts of xenografted mice.
The body weight of xenografted mice was monitored weekly during the treatment period. Blood samples collected at the end of treatment were subjected to cell counting. A. HCT-116-xenografted mice. B. HeLa-xenografted mice. Values are the means ± s.e.m. (n = 6 for HCT-116-xenografted mice, n = 5 for HeLa-xenografted mice). WBCs, white blood cells; RBCs, red blood cells; Hb, hemoglobin; HCT, hematocrit; Plt, platelets.

consistent with our previous results obtained using cultured tumor cell lines [21–23,25,26]. Therefore, GSK-3β activiation and subsequent degradation of β-catenin may be one of important mechanisms underlying the DIF-1 action to inhibit the Wnt/β-catenin target gene expression. However, most colorectal cancers including MAP carry somatic mutations in their *APC* or *β-catenin* genes, which allow β-catenin to escape from GSK-3β-induced degradation and to accumulate in the nuclei, leading to the activation of β-catenin/TCF-mediated gene transcription [28–30]. Indeed, the β-catenin signal is constitutively activated in HCT-116 cells and probably also in the intestinal tumors developed in *Mutyh*$^{-/-}$ mice [11–14,29,30], which may be a reason why DIF-1 could not decrease β-catenin in tumors of *Mutyh*$^{-/-}$ mice and HCT-116 xenograft tumors (Figs. 3B and 5C). Despite constitutively active β-catenin, DIF-1 strongly suppressed the expression of cyclin D1 and TCF7L2 without affecting β-catenin expression levels in the intestinal tumors of *Mutyh*$^{-/-}$ mice and HCT-116-xenograft tumors. This result was consistent with our previous *in-vitro* study using HCT-116, in which we concluded that DIF-1 inhibited "Wnt target" gene expression through inhibition of Egr-1-mediated TCF7L2 gene transcription independent of β-catenin [27]. As shown in the present study, DIF-1 also suppressed the expression of Egr-1 *in vivo*, indicating that DIF-1 may inhibit tumor growth *in vivo* by the same mechanism as revealed *in vitro*.

DIF-1 may have at least three pharmaceutical merits in comparison to existing anti-cancer drugs. First, the mechanisms of its action are very unique. DIF-1 strongly inhibits the Wnt/β-catenin signaling pathway whether APC and/or β-catenin are intact or mutated, resulting in powerful suppression of the expression levels of cyclin D1 and TCF7L2. Although this pathway is often excessively activated in cancer cells, there is few anti-cancer drugs that target this pathway so far. Second, DIF-1 is unlikely to induce serious adverse reactions. DIF-1 induces cell cycle arrest at G_1 phase without affecting cell viability [21,23,25]. In the present *in-vivo* study, repeated administration of DIF-1 did not reduce the body weight or blood cell counts in mice. Certainly, it is unknown whether this cytoprotective property is advantageous in the treatment of cancer, for which cytotoxic drugs are usually used. We expect that DIF-1 is useful at least when used in combination with cytotoxic anti-cancer drugs. Third, DIF-1 can be

applied through the digestive tract, although improvement can be required to prolong its half life in the blood. In summary, DIF-1 may have potential as a novel oral anti-cancer agent with unique mechanisms of action and less toxicity.

In addition, *in-vitro* and *in-vivo* experiments using endothelial cells have shown that DIF-1 inhibits angiogenesis by reducing the expression of vascular endothelial growth factor receptor-2, which is independent of its effect on the Wnt/β-catenin signaling pathway [26]. Therefore, inhibition of the Wnt/β-catenin signaling pathway may not be the only mechanism for the anti-tumor effect of DIF-1. Despite our efforts and those of other research groups, the target molecule(s) of DIFs for its antiproliferative effect on mammalian cells has not yet been identified [40,41]. Identification of the target molecule(s) may not only reveal the precise mechanisms for the antiproliferative effect of DIFs but also offer novel anti-cancer drugs that suppress both tumor cell proliferation and neovascularization.

Acknowledgments

We thank Issei Egashira, Naoya Kubokura, Masaki Arioka and Fumie Shiraishi (Department of Clinical Pharmacology, Faculty of Medical Sciences, Kyushu University) for technical assistance and Minako Hirahashi (Department of Anatomic Pathology, Faculty of Medical Sciences, Kyushu University) for useful discussion. This study was supported by KAKENHI to FTY (21590284 and 25460334).

References

[1] Nelson WJ, Nusse R. Convergence of Wnt, β-catenin, and cadherin pathways. Science 2004;303:1483–7.
[2] Moon RT, Bowerman B, Boutros M, Perrimon N. The promise and perils of Wnt signaling through β-catenin. Science 2002;296:1644–6.
[3] Akiyama T. Wnt/β-catenin signaling. Cytokine Growth Factor Rev 2000;11:273–82.
[4] Sherr CJ. Cancer cell cycles. Science 1996;274:1672–7.
[5] Meyer N, Penn LZ. Reflecting on 25 years with MYC. Nat Rev Cancer 2008;8:976–90.
[6] Barnes DM, Gillett CE. Cyclin D1 in breast cancer. Breast Cancer Res Treat 1998;52:1–15.
[7] Nesbit CE, Tersak JM, Prochownik EV. MYC oncogenes and human neoplastic disease. Oncogene 1999;18:3004–16.
[8] Utsunomiya T, Doki Y, Takemoto H, Shiozaki H, Yano M, Sekimoto M, et al. Correlation of β-catenin and cyclin D1 expression in colon cancers. Oncology 2001;61:226–33.
[9] Fu M, Wang C, Li Z, Sakamaki T, Pestell RG. Minireview Cyclin D1: normal and abnormal functions. Endocrinology 2004;145:5439–47.
[10] Logan CY, Nusse R. The Wnt signaling pathway in development and disease. Annu Rev Cell Dev Biol 2004;20:781–810.
[11] Morin PJ, Sparks AB, Korinek V, Barker N, Clevers H, Vogelstein B, et al. Activation of β-catenin-Tcf signaling in colon cancer by mutations in β-catenin or APC. Science 1997;275:1787–90.
[12] Satoh S, Daigo Y, Furukawa Y, Kato T, Miwa N, Nishiwaki T, et al. AXIN1 mutations in hepatocellular carcinomas, and growth suppression in cancer cells by virus-mediated transfer of AXIN1. Nat Genet 2000;24:245–50.
[13] McDonald SA, Preston SL, Lovell MJ, Wright NA, Jankowski JA. Mechanisms of disease: from stem cells to colorectal cancer. Nat Clin Pract Gastroenterol Hepatol 2006;3:267–74.
[14] Segditsas S, Tomlinson I. Colorectal cancer and genetic alterations in the Wnt pathway. Oncogene 2006;25:7531–7.
[15] Cohen P, Frame S. The renaissance of GSK3. Nat Rev Mol Cell Biol 2001;2:769–76.
[16] Frame S, Cohen P. GSK3 takes centre stage more than 20 years after its discovery. Biochem J 2001;359:1–16.
[17] Diehl JA, Cheng M, Roussel MF, Sherr CJ. Glycogen synthase kinase-3β regulates cyclin D1 proteolysis and subcellular localization. Genes Dev 1998;12:3499–511.
[18] Takahashi-Yanaga F, Sasaguri T. GSK-3β regulates cyclin D1 expression: a new target for chemotherapy. Cell Signal 2008;20:581–9.
[19] Morris HR, Taylor GW, Masento MS, Jermyn KA, Kay RR. Chemical structure of the morphogen differentiation inducing factor from *Dictyostelium discoideum*. Nature 1987;328:811–4.
[20] Morris HR, Masento MS, Taylor GW, Jermyn KA, Kay RR. Structure elucidation of two differentiation inducing factors (DIF-2 and DIF-3) from the cellular slime mould *Dictyostelium discoideum*. Biochem J 1988;249:903–6.
[21] Takahashi-Yanaga F, Taba Y, Miwa Y, Kubohara Y, Watanabe Y, Hirata M, et al. Dictyostelium differentiation-inducing factor-3 activates glycogen synthase kinase-3β and degrades cyclin D1 in mammalian cells. J Biol Chem 2003;278:9663–70.
[22] Yasmin T, Takahashi-Yanaga F, Mori J, Miwa Y, Hirata M, Watanabe Y, et al. Differentiation-inducing factor-1 suppresses gene expression of cyclin D1 in tumor cells. Biochem Biophys Res Commun 2005;338:903–9.
[23] Mori J, Takahashi-Yanaga F, Miwa Y, Watanabe Y, Hirata M, Morimoto S, et al. Differentiation-inducing factor-1 induces cyclin D1 degradation through the phosphorylation of Thr^{286} in squamous cell carcinoma. Exp Cell Res 2005;310:426–33.
[24] Takahashi-Yanaga F, Mori J, Matsuzaki E, Watanabe Y, Hirata M, Miwa Y, et al. Involvement of GSK-3β and DYRK1B in differentiation-inducing factor-3-induced phosphorylation of cyclin D1 in HeLa cells. J Biol Chem 2006;281:38489–97.
[25] Matsuzaki E, Takahashi-Yanaga F, Miwa Y, Hirata M, Watanabe Y, Sato N, et al. Differentiation-inducing factor-1 alters canonical Wnt signaling and suppresses alkaline phosphatase expression in osteoblast-like cell lines. J Bone Miner Res 2006;21:1307–16.
[26] Yoshihara T, Takahashi-Yanaga F, Shiraishi F, Morimoto S, Watanabe Y, Hirata M, et al. Anti-angiogenic effects of differentiation-inducing factor-1 involving VEGFR-2 expression inhibition independent of the Wnt/β-catenin signaling pathway. Mol Cancer 2010;9:245.
[27] Jingushi K, Takahashi-Yanaga F, Yoshihara T, Shiraishi F, Watanabe Y, Hirata M, et al. DIF-1 inhibits the Wnt/β-catenin signaling pathway by inhibiting TCF7L2 expression in colon cancer cell lines. Biochem Pharmacol 2012;83:47–56.
[28] Al-Tassan N, Chmiel NH, Maynard J, Fleming N, Livingston AL, Williams GT, et al. Inherited variants of MYH associated with somatic G:C–>T:A mutations in colorectal tumors. Nat Genet 2002;30:227–32.
[29] Sampson JR, Dolwani S, Jones S, Eccles D, Ellis A, Evans DG, et al. Autosomal recessive colorectal adenomatous polyposis due to inherited mutations of MYH. Lancet 2003;362:39–41.
[30] Sieber OM, Lipton L, Crabtree M, Heinimann K, Fidalgo P, Phillips RK, et al. Multiple colorectal adenomas, classic adenomatous polyposis, and germ-line mutations in MYH. N Engl J Med 2003;348:791–9.
[31] Sakamoto K, Tominaga Y, Yamauchi K, Nakatsu Y, Sakumi K, Yoshiyama K, et al. MUTYH-null mice are susceptible to spontaneous and oxidative stress induced intestinal tumorigenesis. Cancer Res 2007;67:6599–604.
[32] Masento MS, Morris HR, Taylor GW, Johnson SJ, Skapski AC, Kay RR. Differentiation-inducing factor from the slime mould *Dictyostelium discoideum* and its analogues. Synthesis, structure and biological activity. Biochem J 1988;256:23–8.
[33] Traynor D, Kay RR. The DIF-1 signaling system in Dictyostelium. Metabolism of the signal. J Biol Chem 1991;266:5291–7.
[34] Steinbach G, Lynch PM, Phillips RK, Wallace MH, Hawk E, Gordon GB, et al. The effect of celecoxib, a cyclooxygenase-2 inhibitor, in familial adenomatous polyposis. N Engl J Med 2000;342:1946–52.
[35] Ohtsubo T, Nishioka K, Imaiso Y, Iwai S, Shimokawa H, Oda H, et al. Identification of human MutY homolog (hMYH) as a repair enzyme for 2-hydroxyadenine in DNA and detection of multiple forms of hMYH located in nuclei and mitochondria. Nucleic Acids Res 2000;28:1355–64.
[36] Hirano S, Tominaga Y, Ichinoe A, Ushijima Y, Tsuchimoto D, Honda-Ohnishi Y, et al. Mutator phenotype of MUTYH-null mouse embryonic stem cells. J Biol Chem 2003;278:38121–24.
[37] Klungland A, Rosewell I, Hollenbach S, Larsen E, Daly G, Epe B, et al. Accumulation of premutagenic DNA lesions in mice defective in removal of oxidative base damage. Proc Natl Acad Sci USA 1999;96:13300–05.
[38] Sakoguchi-Okada N, Takahashi-Yanaga F, Fukada K, Shiraishi F, Taba Y, Miwa Y, et al. Celecoxib inhibits the expression of survivin via the suppression of promoter activity in human colon cancer cells. Biochem Pharmacol 2007;73:1318–29.
[39] Takahashi-Yanaga F, Yoshihara T, Jingushi K, Miwa Y, Morimoto S, Hirata M, et al. Celecoxib-induced degradation of T-cell factors-1 and -4 in human colon cancer cells. Biochem Biophys Res Commun 2008;377:1185–90.
[40] Matsuda T, Takahashi-Yanaga F, Yoshihara T, Maenaka K, Watanabe Y, Miwa Y, et al. Dictyostelium differentiation-inducing factor-1 binds to mitochondrial malate dehydrogenase and inhibits its activity. J Pharmacol Sci 2010;112:320–6.
[41] Shimizu K, Murata T, Tagawa T, Takahashi K, Ishikawa R, Abe Y, et al. Calmodulin-dependent cyclic nucleotide phosphodiesterase (PDE1) is a pharmacological target of differentiation-inducing factor-1, an antitumor agent isolated from Dictyostelium. Cancer Res 2004;64:2568–71.

SCIENTIFIC REPORTS

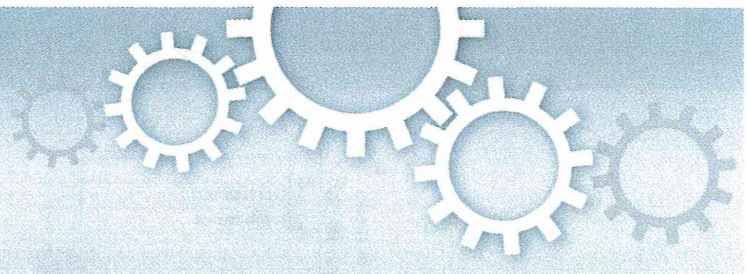

OPEN

SUBJECT AREAS:
EVOLUTIONARY BIOLOGY
MUTATION

Received
8 January 2014

Accepted
28 March 2014

Published
15 April 2014

Correspondence and requests for materials should be addressed to K.S. (sakumi@bioreg.kyushu-u.ac.jp)

8-oxoguanine causes spontaneous *de novo* germline mutations in mice

Mizuki Ohno[1], Kunihiko Sakumi[2,3], Ryutaro Fukumura[4], Masato Furuichi[5], Yuki Iwasaki[6,7], Masaaki Hokama[2], Toshimichi Ikemura[6], Teruhisa Tsuzuki[1], Yoichi Gondo[4] & Yusaku Nakabeppu[2,3]

[1]Department of Medical Biophysics and Radiation Biology, Faculty of Medical Sciences, Kyushu University, Fukuoka 812-8582, Japan, [2]Division of Neurofunctional Genomics, Department of Immunobiology and Neuroscience, Medical Institute of Bioregulation, Kyushu University, Fukuoka 812-8582, Japan, [3]Research Center for Nucleotide Pool, Kyushu University, Fukuoka 812-8582, Japan, [4]Mutagenesis and Genomics Team, RIKEN BioResource Center, Tsukuba 305-0074, Japan, [5]Radioisotope Center, Kyushu University, Fukuoka 812-8582, Japan, [6]Department of Computer Bioscience, Nagahama Institute of Bio-Science and Technology, Nagahama 526-0829, Japan, [7]Research Fellow of the Japan Society for the Promotion of Science.

Spontaneous germline mutations generate genetic diversity in populations of sexually reproductive organisms, and are thus regarded as a driving force of evolution. However, the cause and mechanism remain unclear. 8-oxoguanine (8-oxoG) is a candidate molecule that causes germline mutations, because it makes DNA more prone to mutation and is constantly generated by reactive oxygen species *in vivo*. We show here that endogenous 8-oxoG caused *de novo* spontaneous and heritable G to T mutations in mice, which occurred at different stages in the germ cell lineage and were distributed throughout the chromosomes. Using exome analyses covering 40.9 Mb of mouse transcribed regions, we found increased frequencies of G to T mutations at a rate of 2×10^{-7} mutations/base/generation in offspring of *Mth1/Ogg1/Mutyh* triple knockout (TOY-KO) mice, which accumulate 8-oxoG in the nuclear DNA of gonadal cells. The roles of MTH1, OGG1, and MUTYH are specific for the prevention of 8-oxoG-induced mutation, and 99% of the mutations observed in TOY-KO mice were G to T transversions caused by 8-oxoG; therefore, we concluded that 8-oxoG is a causative molecule for spontaneous and inheritable mutations of the germ lineage cells.

Evolution requires *de novo* germline mutations that are newly generated in germ lineage cells and inheritable to the offspring. It is evident that germline mutations occur, because sporadic and deleterious mutations that cannot be transmitted to offspring continuously appear in human populations[1–4]. The human *de novo* germline mutation rate is estimated to be 1.20×10^{-8}/nucleotide/generation[1]. However, the cause and mechanism of mutations in the germ cell lineage remain unclear. We hypothesized that the cause of these mutations would be endogenously and spontaneously generated and remain in the germ cell lineage. 8-oxoG is one of the candidate molecules for causing germline mutation, because it is endogenously generated by reactive oxygen species (ROS) derived from cellular respiration, constitutively exists in DNA[5] and is known to cause G to T and A to C transversion mutations by the ability to pair with A as well as C during DNA replication[6–8].

Mammals possess three enzymes to avoid 8-oxoG-induced mutations. MTH1 (*mutT* homologue 1, NUDT1) degrades 8-oxodGTP in the nucleotide pool to prevent its incorporation into DNA[9]. OGG1 (8-oxoG DNA glycosylase) excises 8-oxoG from DNA[10,11], and MUTYH (*mutY* homologue, adenine DNA glycosylase) removes adenine misincorporated opposite 8-oxoG in DNA[12]. We and other groups have reported that mice deficient in these enzymes are prone to developing cancer, indicating a mutator phenotype in somatic cells[13–16]. MUTYH is also responsible for MUTYH-associated polyposis in humans[17].

To evaluate the contribution of 8-oxoG to *de novo* germline mutation, we established the *Mth1/Ogg1/Mutyh* triple knockout (TOY-KO) mice, in which unrepaired endogenous 8-oxoG accumulates in the genome DNA. In this paper, using the TOY-KO mice, we showed that 8-oxoG causes G to T mutations in germ lineage cells (Supplementary Fig. S1 online).

Results

Spontaneous mutations increased in *Mth1*$^{-/-}$/*Ogg1*$^{-/-}$/*Mutyh*$^{-/-}$ (TOY-KO) mice. To evaluate the contribution of 8-oxoG to *de novo* germline mutation, we established the TOY-KO mouse in the C57BL/6J background (>N16). TOY-KO mice are viable and fertile, although increased amounts of 8-oxoG accumulated in various tissues, including the gonads (Fig. 1a). Moreover, TOY-KO mice had a shorter lifespan (Fig. 1b) and developed various types of tumors (Fig. 1c). We maintained the TOY-KO mouse line originating from one pair

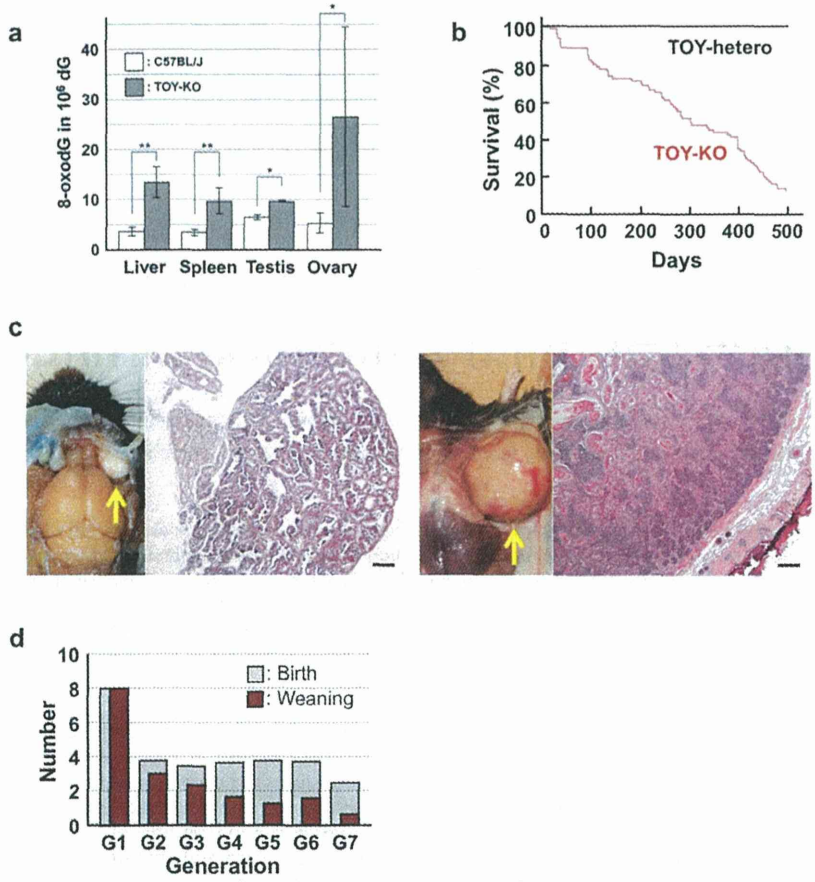

Figure 1 | Phenotype of TOY-KO mice. (a) Accumulation of 8-oxodG in TOY-KO mouse tissues. LC-MS/MS was used to determine the amount of 8-oxodG[29]. Data are presented as the means ± SD. Wilcoxon tests were used to analyze differences between TOY-KO (gray) and C57BL/6J:Jcl (open) mouse tissues (* $P < 0.05$; ** $P < 0.001$). (b) Survival of TOY-KO mice. The survival curve of TOY-KO mice (n = 56, indicated in red) was compared with that of *Mth1*$^{+/-}$/*Ogg1*$^{+/-}$/*Mutyh*$^{+/-}$ (TOY-hetero) mice (n = 14, indicated in black). (c) A Harderian gland tumor (left) and a trichoepithelioma (right) observed in a TOY-KO mice (indicated by arrows). Hematoxylin and eosin staining of each tumor is shown. Scale bars, 200 μm. (d) Numbers of newborn and weaned mice. Gray and red bars indicate the numbers of newborn and weaned mice in each generation of TOY-KO mice, respectively.

(G1) to the 8th generation (G8) by intragenerational mating (Supplementary Fig. S2 online). More than 35% of TOY-KO mice carried macroscopically distinguishable tumors (Supplementary Fig. S2 online). As the generations increased, it became difficult to obtain mice for breeding because of the decreased number of weaned mice (Fig. 1d). Several phenotypic variations were found among the progeny, such as hydrocephalus, belly white spot and anophthalmia (Supplementary Fig. S2 online). In cases of hydrocephalus and white spot, the traits were transmitted to the next generation in an autosomal dominant fashion with incomplete penetrance (Fig. 2, Supplementary Fig. S2 online). These features indicate that heritable mutations could arise in the TOY-KO mice.

To detect mutations that occur in the germ cell lineage and are transmitted across generations of TOY-KO mice, we performed whole exome sequencing analysis (Fig. 3a). We searched for different sequences between the C57BL/6J mouse reference genome (MGSC-v37) and TOY-KO mice that belonged to the most advanced generation of each branch of the pedigree (TOY365F, TOY609F and TOY450F, shown in Fig. 3b). No sequencing reads corresponding to parts of the wild-type reference sequences of targeted *Mutyh*, *Mth1*, and *Ogg1* loci were obtained in chromosomes 4, 5, and 6, respectively (Supplementary Fig. S3 online), which confirmed that the TOY-KO mouse was indeed deficient for the three genes, and validated our exome analysis. By analyzing the exome covering 40.9 Mb of mouse transcribed sequences, which included 19,427 genes from 17 chromosomes, excluding chromosomes 4, 5, and 6 from the analysis to avoid ambiguity, we identified 262 base substitution mutations (Fig. 3c, Supplementary Table S1 online, Supplementary Data S1 online). No insertion/deletion mutations were detected in this analysis.

Identification of mutation origin mice. The 262 mutations detected in TOY365F, TOY609F and TOY450F had occurred in one of the mice in the 8-generations of the pedigree (Fig. 3b); therefore, we determined the mutation origin mouse that initially possessed the mutated allele in its tail DNA. We traced each mutation on the pedigree by determining the sequences of all mutated alleles in 35 TOY-KO mice shown in the pedigree (Fig. 3b), using MassArray or Sanger's sequencing, and identified the origin of each *de novo* mutation. The results of the sequencing are summarized in Supplementary Data S1 online with annotations. Among them, we considered that 247 mutations found in G2–G8 mice had spontaneously occurred in the germ cell lineage of TOY-KO mice, because these mutated alleles were derived from gametes of their parent mice (G1–G7) or were generated during early development of the mice (G2–G8). The spectrum of germline mutation observed in TOY-KO mice indicated a distinct feature: 99% (244/247) of the mutations were G to T transversions (Table 1). G to T mutations had specifically increased in TOY-KO mice lacking the ability to avoid 8-oxoG-induced mutations; therefore, we concluded that 8-oxoG is a causative